



Contents lists available at: <http://qu.edu.iq>

Al-Qadisiyah Journal for Engineering Sciences

Journal homepage: <https://qjes.qu.edu.iq>



Research Paper

Mechanical properties of functionally graded Al-Cr-Fe alloy fabricated by sequential casting with influence of vibration

Abdul Raheem Kadhim Abid Ali  , **Haydar Al-Ethari** , and **Ali Abbas Hasan** 

Department of Metallurgical Engineering, Materials Engineering College, University of Babylon, Babylon, Iraq.

ARTICLE INFO

Article history:

Received 24 June 2024

Received in revised form 27 September 2024

Accepted 12 April 2025

keyword:

Aluminum alloy
Sequential casting
Vibration moled
Finer granular
Interface
Automotive pistons

ABSTRACT

The performance of functionally graded materials is much better than materials with unchanged properties and compositions. Al-Cr-Fe alloys with different Cr concentrations were proposed for this work. Potential applications for these materials include automotive pistons. FGM was fabricated by successive stages of the sequential casting method with mechanical vibration during the solidification. FGM sample consists of two alloys with different chemical composition (Al-8Si-2Fe), and (Al-2Cr-2Fe). Two types of samples were studied and compared, with and without mold vibration. The method of mechanical mold vibration, which in turn reduces the segregation and pores in the cast and refines the microstructure. The results of the XRD showed the presence of α - Al phase, $Al_{80}Cr_{13.5}Fe_{6.5}$, $Al_{13}Cr_2$ and $Al_{13}Fe_4$ compounds that enhance the strength of the alloy. Optical microscope images showed a difference in the microstructure on both sides of the interface between the two alloys. There is variation in the hardness values due to the difference in the chemical composition of the alloys. The recorded improvement in the tensile strength was 17%, and the decrease in Compression by 1.5%.

© 2025 University of Al-Qadisiyah. All rights reserved.

1. Introduction

Functionally graded materials are advanced composite materials utilized in engineering that exhibit a spatial variation in composition and/or structure to meet specific requirements. FGMs can be classified into three categories based on their characteristics: chemical composition gradient, microstructural gradient, and porosity gradient [1]. Functionally graded materials, FGMs, are characterized by a gradual change in their chemical composition throughout the material. Microstructural gradient fiber-reinforced composites display a distinct and easily observable variation in their microstructure, as listed by [2]. These materials are used in a wide range of sectors, including aerospace, nuclear, electrical, medical, military, and automotive.

Aluminum alloys, in particular, are often used in the automobile industry as a result of more stringent environmental regulations [3]. Cast aluminum alloy components, such as pistons, engine blocks, and rocker covers, are often found in ordinary automobiles. Aluminum alloys are regarded as sustainable materials because they can be recycled, are cost-effective, lightweight, weldable, and possess strong mechanical properties [4]. The FGMs can be produced using many methods, such as gas-based, liquid-phase, and solid-phase techniques [5]. Centrifugal casting, squeeze casting, gravity casting, investment casting, and sintering are commonly used methods for producing metallic functionally graded materials [6]. Gravity casting is a simple method used in the casting process to produce FGMs. This process employs a resilient mold, often constructed from steel. The mold is coated with a protective paint and then heated to a desired temperature, which enables the removal of the cast. The cast production sequence consists of many discrete steps: (i) cleansing the mold; (ii) executing the casting procedure; (iii) removing the cast; and (iv) severing the sprue [7].

Aluminum-transition metal alloys have exceptional stability at relatively high temperatures, making them highly suitable for many automotive and aerospace

applications that need lightweight alloys with high strength and a wide operating temperature range [8]. Chromium, Cr, is considered one of the most intriguing alloying elements for developing dispersion-hardened Aluminum alloys, Al, that remain stable at high temperatures. This is because Cr has poor solubility and low diffusivity in solid Al [9]. Al-Cr-Fe alloys is characterized by a unique combination of bulk and surface properties such as low surface energy, increasing electrical conductivity with temperature, combined with low thermal conductivity, high hardness, low adhesion/friction coefficient and good corrosion resistance down to very low pH (acidic/basic) values (0–2) [10], which should be acceptable for many practical applications. In addition, Ferritic-structure Al-Cr-Fe alloys exhibit good oxidation resistance and can be used as accident-tolerant light water reactor fuel cladding [11, 12]. Recent research has shown that gravity casting is a viable technique for producing aluminum-FGM pistons with two different compositions, resulting in improved mechanical strength and ductility [11]. The presence of silicon in these alloys might influence their resistance to wear and fatigue cracking [12]. Ensuring the strength of the link between alloys in Functionally Graded Materials is of high importance in the automotive industry. This necessitates a comprehensive examination via micro-hardness tests, impact testing, and investigation of the material's microstructure using Scanning Electron Microscopy (SEM) [13]. Researchers have investigated the use of vibration in the casting process to inject energy into the material, resulting in advantages such as grain refinement and defect reduction. Sequential stir casting with solidification under mechanical vibration is a technique used to produce functionally graded materials (FGMs) employing aluminum-silicon and aluminum-chromium alloys [14]. When looking at the use of FGM in automotive applications, particularly with regard to aluminum alloys, which are often used in this sector [15], it is indeed feasible to integrate the notion of FGM with aluminum alloys [16]. In this technique, the specimens are tested with a mechanical vibration setup.

* Corresponding Author.

E-mail address: mat.abdulraheem.k@uobabylon.edu.iq; Tel: (+964) 781 811-8508 (Abdul Raheem Abid Ali)



Nomenclature

| | | | |
|-------|-------------------------------|-------|---|
| A_1 | Sample 1 | L | Total length of lines (μm) |
| A_2 | Sample 2 | N | Total number of granules in which lines pas |
| FGM | Functionally graded materials | UTS | Ultimate tensile strength |
| HF | Hydrofluoric | XRD | X-ray diffraction |
| HV | Vickers hardness | | |

The outline of the experiment is shown in Fig. 1 where the mold is cemented rigidly on a vibratory table, the table is rigidly coupled to the vibration exciter, which generates vibrations at different frequencies of oscillation and transmits them to the table and molds. The system is turned to vibrate at different frequencies of oscillation. The molten metal solidifies under these vibratory conditions [17]. Chernov used mechanical vibration tests during solidification of steel and observed that the final structure of primary austenite was refined and the mechanical properties improved [18].

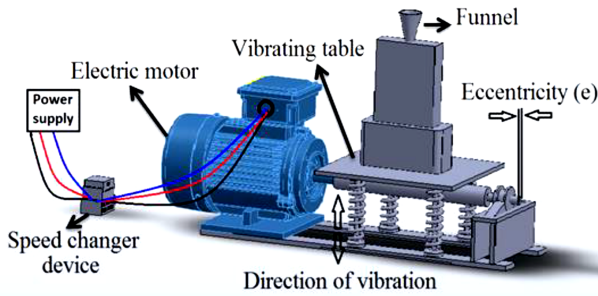


Figure 1. Sketch of vibration device [19].

The mechanical vibrations technique is a common promising technique that is used during the solidification of molten in spite of it restricted the operator [20]. These techniques have low cost, simply system, no complexity in the production of casting and are easy to hold compering with ultrasonic and electromagnetic methods [21–24]. The methods of applying mechanical vibration can be classified into two types. First, mechanical vibration is introduced into the solidifying metals under continuous cooling during casting [25]. It has been revealed that mechanical vibration has strong effects on the final ingot or cast component, such as grain refinement, degassing, and mechanical properties. Second, mechanical vibration is used to treat a molten alloy at various solid fractions in the mushy zone. It has been shown that semi-solid slurry or billet could be produced [26,27].

2. Materials and methods

2.1 Al-Cr-Fe alloys sample preparation

Pieces of aluminum wire were melted in the ceramic crucible and maintained at 900°C. The Chromium and iron powders in progressive quantities were added gradually to the melt. The powders were divided into parts, each of which was enveloped by aluminum foil heated to 300°C before adding to the melt. Table 1 listed the chemical composition of Al-Cr-Fe alloys. Chemical analysis is done by metal analysis SPECTRO model [3].

Table 1. Chemical composition of Al-Cr-Fe alloys.

| Element | Cr | Fe | Mn | Mg | Ti | Al% |
|---------|-------|-------|--------|--------|-------|------|
| A1 | 8.000 | 1.930 | 0.0198 | 0.0267 | 0.002 | Bal. |
| A2 | 2.000 | 2.000 | 0.0142 | 0.0224 | 0.005 | Bal. |

2.2 Fabrication of the FGM alloy samples

The FG alloy samples were fabricated based on the prepared alloy samples. Two casting procedures were employed to fabricate two groups of castings. The first was cast under the effect of mechanical vibration, the second was cast without such effect. The mechanical vibrations were provided using a vibrating device shown in Fig. 2. The device provides the vibrations to the shaft with an eccentricity (e) (1.50 mm). The shaft can be rotated at a rotating speed of (900 rpm) to get the required frequency [16]. Due to the eccentricity, a table where the die is attached to the device can be moved vertically with the designed amplitude, which is equal to the eccentricity. The FGM alloys were produced using a process of sequential gravity casting, where the first composition was casted first, followed by the second composition. The time

interval between the two casting processes and the pouring temperature were set to 20 seconds and 900 °C, respectively.

Three varieties of FGM castings were manufactured. The types are Al-8at.%Cr-2at.%Fe and Al-2at.%Cr-2at.%Fe. During the casting process, the temperature of the alloy was elevated beyond its liquid state. The molten substance was introduced into a steel mold that had been preheated and had a cylindrical chamber of 24 mm in diameter and 150 mm in height. The temperature of the mold was raised to 400°C. In order to achieve casting under the influence of vibrations, mechanical vibrations are initiated prior to pouring and are maintained until the solidification process is fully completed.



Figure 2. Vibration device used in the practical aspect.

3. Experimental lab work

3.1 X-ray Diffraction (XRD)

Specimens with (20 × 10 mm) at the interface zone were prepared for X-ray diffraction analysis. The measurement conditions are Target: Cu, wavelength of 1.54060 v, and currents are 30 KV and 15 mA respectively. The scanning step of 0.05 with a step time of 2 sec. and a scanning range of (5°-80°) was used, the XRD device type AERIS [17].

3.2 Optical microscope analyses

The test was conducted on the produced FGM sample specimens, measuring 130 mm in length were used. The specimen was flattened by employing SiC grinding sheets with varying roughness levels (400, 800, 1000, 1200, and 2000 grit size). The grinding and polishing procedures were carried out utilizing the MP-2B grinder polisher machine. The Al-Cr-Fe alloy specimens were subjected to etching using a solution of 5 ml of hydrofluoric acid (HF) and 195 ml of distilled water for a duration of 15 seconds [19]. Subsequently, the specimens were rinsed with distilled water and dried using an electric dryer. A specimen’s microstructure was examined using an optical microscope at a magnification of 400X. Experiments were performed at ambient temperature with a compression rate of 0.5 millimeters per minute.

3.3 Grain size measurement

It is usually favored to determine the size of the grain through the linear intercept technique as shown in Fig. 3. Through this technique, using photographic pictures of samples, draw lines on a photomicrograph, as in the Eq. 1 [21]. Several lines should be drawn to obtain the accurate result as shown in Fig. 3.

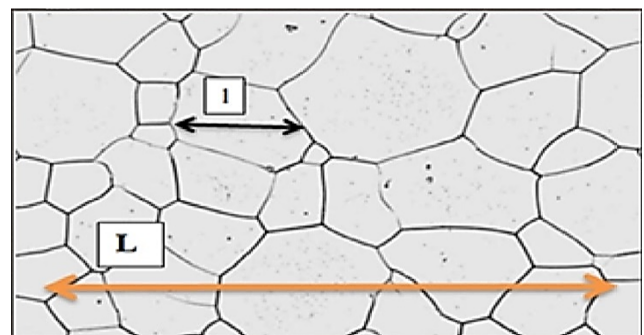


Figure 3. Intercept Method of Determining Grain Size [21]

$$l = \frac{L}{N} \quad (1)$$

Where the number on the left side of Eq. 1 is the grain size which is l (μm), L is the total length of line (μm), and N is the total number of granules in which line pas.

3.4 Vickers hardness test

The Vickers hardness test was carried out according to ASTM-E10-15a, with a load of 10 Kg. Appropriate grinding and polishing were carried out before subjecting the specimens to the test. The test was performed at every 5 mm along the specimen's length of 130 mm. At the interface region, the tests were carried out at every 0.25 mm. The test was carried out via a hardness tester type (HVS-1000). Tests were conducted at room temperature with the rate of compression 0.5 (mm/min) [7].

3.5 Tensile test

Standard specimens were prepared with dimensions according to ASTM-E8 standard as shown in Fig. 4 [1]. Computer-controlled universal testing machine model (WDW) was used with a loading rate of 0.2 (mm/min) at room temperature. Experiments were performed at standard room temperature with a compression rate of 0.5 (mm/min), this work was done on the AGX-V machine.

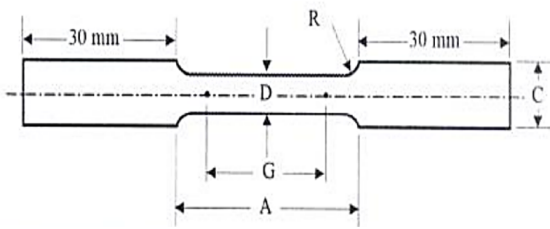


Figure 4. Tensile test specimens standard [1].

3.6 Compression test

Compression test specimens were fabricated from the cast alloy samples. The specimens possessed a configuration and dimensions of 23 mm in diameter and 46 mm in height, with the interface positioned in the center as per the ASTM-E8M-04 standard. The compression tests were performed at ambient temperature at a speed of 0.5 (mm/min) using device type AGX-V.

4. Results and discussion

4.1 XRD analyses

The charts of the XRD for the sample in the zone of that functionally graded material were fabricated by casting two different alloys. Peaks match with the standard chart of the X-ray diffraction for each phase are shown in Fig. 5. The XRD for the FGM sample with vibration, there is no difference between the alloy with and without vibration in components, the result including α -Al phase, $\text{Al}_{80}\text{Cr}_{13.5}\text{Fe}_{6.5}$, $\text{Al}_{13}\text{Cr}_2$ and $\text{Al}_{13}\text{Fe}_4$.

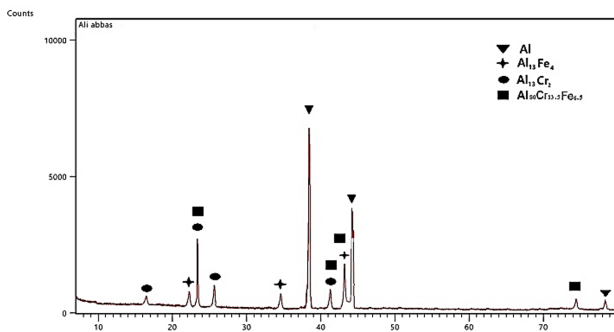


Figure 5. Sketch of vibration device.

4.2 Microstructure

Figure 6 shows the microstructure of samples with vibration, and Fig. 7 without vibration. During solidification, in the separation zone, there are differences that can be identified by the microstructure on both sides of the zone, where the grain shape and matrix interpenetration are different. This is due to the different chemical composition of the alloys. Also, the samples with vibration

effect have a smaller grain size. The absence of pores that appear in the samples without vibration effect indicates the presence of dark spots. In each sample, there is no loss of contact or solubility between the two alloy surfaces.

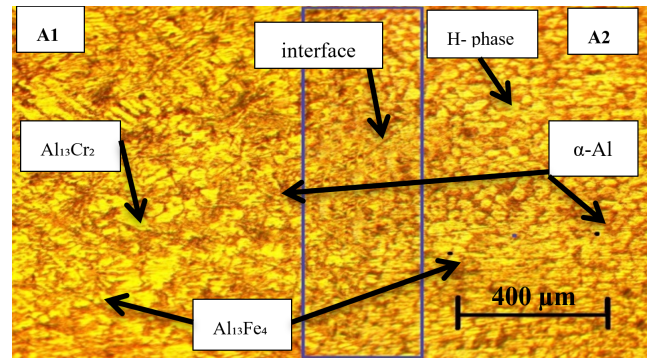


Figure 6. Microstructures without vibrations.

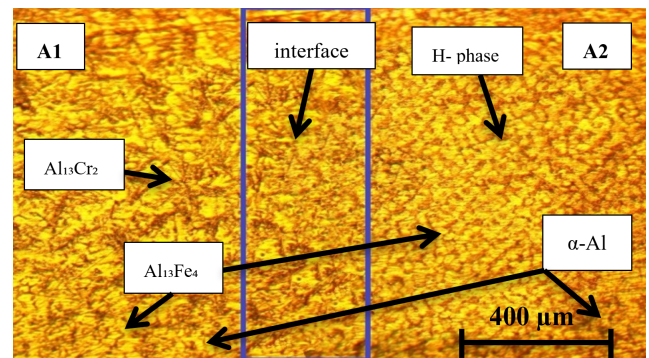


Figure 7. Microstructures with vibrations.

In both forms, the $\text{Al}_{80}\text{Cr}_{13.5}\text{Fe}_{6.5}$ phase appears in a circular shape, while the $\text{Al}_{13}\text{Cr}_2$. The phase appears in the form of large equiaxed particles, while the $\text{Al}_{13}\text{Fe}_4$ phase appears in the form of small equiaxed crystals compared to the $\text{Al}_{13}\text{Cr}_2$ phase, which is a common phase in the two alloys [13].

4.3 Grain size test output

After conducting tests on the grain size, photographic images were taken of sample (a) without vibrations and sample (b) with vibrations. The results are listed in Table 2. The vibration induces refinement by altering the size and distribution of intermetallic particles. The refinement of the casting is influenced by the cooling rate, which is expedited by vibration. This vibration causes the particles to move from the mold walls to the center of the casting, where they act as new nucleation sites. As a result, the overall nucleation rate increases while the growth rate of the reinforced particles decreases.

Table 2. Grain size of Al-Cr-Fe alloys.

| Sample | Grain size (μm) without vibrations | Grain size (μm) with vibrations | Percentage Reduction % |
|--------|---|--|------------------------|
| A1 | 38.10 | 37.98 | 00.05 |
| A2 | 30.40 | 29.10 | 00.04 |

4.4 Vickers hardness test

Figure 8 shows the results of Vickers hardness test conducted on alloy samples. It was found that with increasing chromium content in the alloy, the hardness increases significantly. Using vibration during casting increases the hardness. Alloy A2 has a higher level of hardness compared with sample A1 in Al-Cr-Fe alloy. The fineness of the grain size and the absence of defects and gaps that reduce the hardness values and weaken the matrix can be attributed to. Figure 9 shows the Vickers hardness along the length of the samples, where there is a change in the hardness value for both bars at the joint area at the meeting point of the two surfaces due to the difference in the chemical composition of the alloys. It is noted that the hardness values of the sample under the influence of vibration are almost equal along the length of one alloy, and there is no change in the values as observed in the samples without the influence of vibration.

However, the difference in the hardness values of the one alloy under the influence of vibration is small, as we notice the absence of oscillation along the length of the sample.

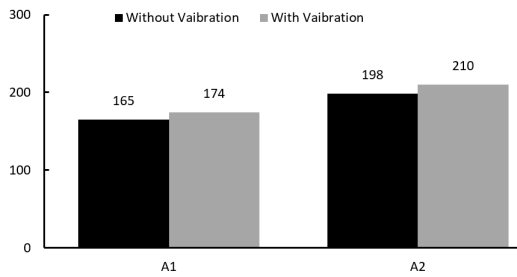


Figure 8. Maximum hardness value.

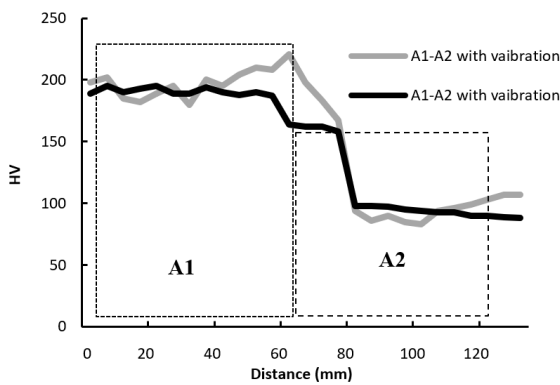


Figure 9. Vickers hardness along the length of the samples.

4.5 Tensile testing

The results of the tensile test are shown in Table 3. The vibration of the samples showed values of 203 MPa with an elongation of 0.11%, while the samples without vibration reached 187 MPa with an elongation of 0.94%. This is due to the strengthening of the $\alpha - Al$ matrix by uniformly distributed compounds inside the alloy. In addition, the $Al_{11}Cr_2$ and $Al_{13}Fe_4$ phases have a strong interconnection between the phases and the matrix. Figure 10 shows the FGM sample before and after the tensile test and Fig. 11 shows the FGM sample after the tensile test. It is noted that in both cases the fracture is in the A2 alloy region due to the weakness of the matrix, as the high chromium value enhances the strength of the matrix, as the compounds are well intertwined.

Table 3. Tensile tested rustle.

| Sample | UTS MPs with vibration | UTS MPs without vibration | Elongation% with vibration | Elongation % without vibration |
|--------|------------------------|---------------------------|----------------------------|--------------------------------|
| A1-A2 | 203 | 187 | 0.11 | 0.94 |



Figure 10. Tensile samples before test .

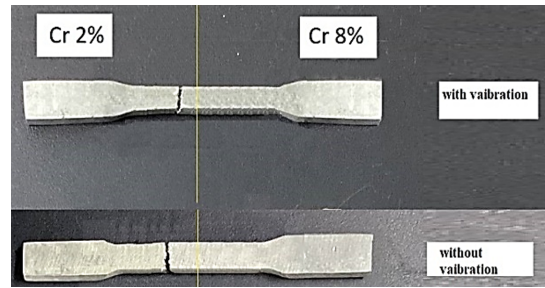


Figure 11. Tensile samples after test .

Table 4. Compression results.

| Sample | Compression MPs with vibration | Compression MPs without vibration |
|--------|--------------------------------|-----------------------------------|
| A1-A2 | 294 | 297 |

4.6 Compression test rustles

The results of compression of samples are shown in Table 4, for samples under vibration and without vibration. All alloy and FGM samples showed lower compression values without using vibration. This is due to the change in grain size and the lack of pores inside the alloy.

5. Conclusions

This study involved the production of innovative forms of FGM through the manipulation of successional casting techniques. The alloy consisting of 8% Chromium and 2% Iron, together with the alloy consisting of 2% Chromium and 2% Iron, was used to produce castings that exhibited high quality and minimal retained flaws. The presence of Fe was considered in order to enhance the mechanical characteristics of the as-cast FGM, particularly by the nucleation of η $Al_{11}Cr_2$, $Al_{13}Fe_4$. Functionally graded materials were castings that were made and then subjected to mechanical vibration testing. The sequential casting method is an effective method for producing materials with graded properties on a similar basis.

- The difference in microscopic structure is due to the difference in the concentration of chromium, which forms compounds with the presence of aluminum and iron.
- The XRD test showed the presence of compounds that would enhance the matrix.
- Vibrations have a positive effect on the plumbing process, as it is reflected in the refine grains, a defect-free structure, and a homogeneous distribution of compounds and elements, which leads to an improvement in mechanical properties.
- In the tensile and compression test, samples under the influence of vibration gave higher values than samples without vibration.

Authors' contribution

All authors contributed equally to the preparation of this article.

Declaration of competing interest

The authors declare no conflicts of interest.

Funding source

This study didn't receive any specific funds.

Data availability

The data that support the findings of this study are available from the corresponding author upon reasonable request.

REFERENCES

[1] K. A. S. W. J.-P. E. A. . R. L. E. Botero, C., "Functionally graded steels obtained via electron beam powder bed fusion," *Key Engineering Materials*, vol. 964, pp. 79–84, November 2023. [Online]. Available: <https://doi.org/10.4028/p-xaC6qO>

- [2] P. W. D.-B. A. G. P. S. A. . B. R. Młynarek-Żak, K., “Structure and selected properties of al–cr–fe alloys with the presence of structurally complex alloy phases,” *Scientific Reports*, vol. 12, no. 1, p. 14194, 2022. [Online]. Available: <https://doi.org/10.1038/s41598-022-17870-0>
- [3] Y. W. Z. Y. L.-C. Q. Y. N. S. . . Y. B. Li, R., “Effect of phase proportion on wear behavior of al–cr–fe–ni dual-phase high entropy alloys,” *Metallography, Microstructure, and Analysis*, vol. 10, no. 2, pp. 106–115, 2021. [Online]. Available: <https://doi.org/10.1007/s13632-020-00709-3>
- [4] L. J. X. F. Z.-L. . Z. Y. Yang, S., “Revisit the vec rule in high entropy alloys (heas) with high-throughput calphad approach and its applications for material design—a case study with al–co–cr–fe–ni system,” *Acta Materialia*, vol. 192, pp. 11–19, 2020. [Online]. Available: <https://doi.org/10.1016/j.actamat.2020.03.039>
- [5] C. E. G. A.-. d. S. C. A. Ribeiro, T. M., “The effects of cr addition on microstructure, hardness and tensile properties of as-cast al–3.8 wt.”
- [6] K. A. H. R.-W. B. K. S. R. J. . M. P. H. Koller, C. M., “Oxidation behavior of intermetallic al–cr and al–cr–fe macroparticles,” *Journal of Vacuum Science Technology*, vol. 35, no. 6, p. 414, 2017. [Online]. Available: <https://doi.org/10.2139/ssrn.4705444>
- [7] M. L. K.-C. S. . G. P. de Araujo, A. P., “Microstructure, phase formation and properties of rapid solidified al–fe–cr–ti alloys,” *Materials Science and Technology*, vol. 36, no. 11, pp. 1205–1214, 2020. [Online]. Available: <https://doi.org/10.1080/02670836.2020.1763555>
- [8] T. E. K. L. . K. V. Švecová, I., “Possibilities of predicting undesirable iron intermetallic phases in secondary al–alloys,” *Transportation Research Procedia*, vol. 55, no. 1, pp. 797–804, 2021. [Online]. Available: <https://doi.org/10.1016/j.trpro.2021.07.047>
- [9] L. S. . R. M. Fracchia, E., “Case study of a functionally graded aluminum part,” *Applied Sciences*, vol. 8, no. 7, p. 1113, 2018. [Online]. Available: <https://doi.org/10.3390/app8071113>
- [10] G. F. S. R. M. A. G. M. B. J. . B. R. Fracchia, E., “Junction characterization in a functionally graded aluminum part,” *Materials*, vol. 12, no. 21, p. 3475, 2019. [Online]. Available: <https://doi.org/10.3390/ma12213475>
- [11] L. Z. Z. Y. Q. J. . L. X. G. Gao, T., “Phase evolution of -al 5 fesi during recycling of al–si–fe alloys by mg melt,” *International Journal of Metalcasting*, vol. 13, no. 2, pp. 473–478, 2019. [Online]. Available: <https://doi.org/10.1007/s40962-018-0279-3>
- [12] L. S. B. X. Z. X. . H. X. Wang, J., “Oxidation behavior of fe–al–cr alloy at high temperature: Experiment and a first principle study,” *Vacuum*, vol. 173, no. 5, p. 109144, 2020. [Online]. Available: <https://doi.org/10.1016/j.vacuum.2019.109144>
- [13] A. F. E. A. G. S. I. C. . C. B. Galano, M., “Nanoquasicrystalline al–fe–cr-based alloys. part ii. mechanical properties,” *Acta materialia*, vol. 57, no. 17, pp. 5120–5130, 2009. [Online]. Available: <https://doi.org/10.1016/j.actamat.2009.07.009>
- [14] W. Y. M. C. L. F. C. X. J. Z. X. . F. Z. Que, Z., “Understanding fe-containing intermetallic compounds in al alloys: an overview of recent advances from the lime research hub,” *Metals*, vol. 12, no. 10, p. 1677, 2022. [Online]. Available: <https://doi.org/10.3390/met12101677>
- [15] L. Z. Z. Y. Q. J. . L. X. Gao, T., “Phase evolution of -al 5 fesi during recycling of al–si–fe alloys by mg melt,” *International Journal of Metalcasting*, vol. 13, no. 2, pp. 473–478, 2019. [Online]. Available: <https://doi.org/10.1007/s40962-018-0279-3>
- [16] . K. V. V. Sheshukov, O. Y., “Influence of titanium and zirconium on the structure and heat-resistance of low-carbon iron–aluminum alloys. steel in translation,” *Izvestiya Ferrous Metallurgy*, vol. 64, no. 9, pp. 621–626, 2021. [Online]. Available: <https://doi.org/10.17073/0368-0797-2021-9-685-692>
- [17] L. B. R. W. B. Y. Q. . Z. N. Q. Chen, H. Z., “Corrosion behaviours of iron–chromium–aluminium steel near the melting point of various eutectic salts,” *Solar Energy Materials and Solar Cells*, vol. 210, no. 19, p. 110510, 2020. [Online]. Available: <https://doi.org/10.1016/j.solmat.2020.110510>
- [18] B. K. P. T. . R. R. Behrens, B. A., “Investigation on the microstructure of ecap-processed iron–aluminium alloys,” *Materials*, vol. 14, no. 1, p. 219, 2021. [Online]. Available: <https://doi.org/10.3390/ma14010219>
- [19] K. D. T. E. G. E. . S. A. Siekaniec, D., “Optimisation of solidification structure and properties of hypoeutectic chromium cast iron,” *Materials*, vol. 15, no. 18, p. 6243, 2022. [Online]. Available: <https://doi.org/10.3390/ma15186243>
- [20] B. A. S. M. R. A. . W. Babilas, R., “Structure and corrosion resistance of al–cu–fe alloys,” *Progress in Natural Science: Materials International*, vol. 30, no. 3, pp. 393–401, 2020. [Online]. Available: <https://doi.org/10.1016/j.pnsc.2020.06.002>
- [21] M. A. S. D. F. M. S. . C.-J. C. M. Pérez-Prado, M. T., “An al-5fe-6cr alloy with outstanding high temperature mechanical behavior by laser powder bed fusion,” *Additive Manufacturing*, vol. 55, no. 0, p. 102828, 2022. [Online]. Available: <https://doi.org/10.1016/j.addma.2022.102828>
- [22] K. A. D. V. K. S. R. J. . M.-P. H. Koller, C. M., “On the oxidation behavior of cathodic arc evaporated al–cr–fe and al–cr–fe–o coatings,” *Journal of Vacuum Science Technology A*, vol. 163, no. 4, pp. 1–9, 2019. [Online]. Available: <https://doi.org/10.1016/j.vacuum.2019.01.052>
- [23] E. M. H. . N. A. H. W. Sourani, F., “On the in situ synthesis of (fe, cr) al and (fe, cr) al–al₂O₃ nanostructured materials,” *Materials Research Express*, vol. 6, no. 8, p. 0850c9, 2019. [Online]. Available: <https://doi.org/10.1088/2053-1591/ab24f5>
- [24] U. A. I. P. S. D. S. A. . T. V. O. Skorodzievskii, V. S., “Dissipative properties of al-(fe, cr) vacuum coatings with different composite structures,” *Surface and Coatings Technology*, vol. 367, no. 1, pp. 179–186, 2019. [Online]. Available: <https://doi.org/10.1016/j.surfcoat.2019.03.074>
- [25] A. H. R. S. A. H. M. J. A. F. A. M. . A. A. Muneer, B. A. I. G., “Thermal stability of nanocrystalline al 10fe 5cr bulk alloy,” *Transactions of Nonferrous Metals Society of China*, vol. 29, no. 2, pp. 242–252, 2019. [Online]. Available: [https://doi.org/10.1016/S1003-6326\(19\)64933-2](https://doi.org/10.1016/S1003-6326(19)64933-2)
- [26] E. I. P. M. . M. L. Shockner, R., “Systematic study of the effect of cr on the microstructure, phase content and hardness of the alcrxfeconi alloys,” *Journal of Alloys and Compounds*, vol. 940, no. 10, p. 168897, 2023. [Online]. Available: <http://doi.org/10.1016/j.jallcom.2023.168897>
- [27] J. A. F. R. S. D. V. S. S. W. A. . M. G. Shi, H., “Compatibility and microstructure evolution of al–cr–fe–ni high entropy model alloys exposed to oxygen-containing molten lead,” *Corrosion Science*, vol. 189, p. 109593, 2021. [Online]. Available: <https://doi.org/10.1016/j.corsci.2021.109593>

How to cite this article:

Abdul Raheem Kadhim Abid Ali, Haydar Al-Ethari, and Ali Abbas Hasan. (2025). 'Mechanical properties of functionally graded Al-Cr-Fe alloy fabricated by sequential casting with influence of vibration', *Al-Qadisiyah Journal for Engineering Sciences*, 18(2), pp. 126-130. <https://doi.org/10.30772/qjes.2024.151081.1280>